Image Color Space Transform with Enhanced KLT

Roumen Kountchev and Roumiana Kountcheva

Abstract. The use of the Karhunen-Loève Transform (KLT) for the processing of the image primary color components gives as a result their decorrelation, which ensures the enhancement of such operations as: compression, color-based segmentation, etc. The basic problem is the high computational complexity of the KLT. In this paper is offered a simplified algorithm for the calculation of the KL color transform matrix. The presented approach is based on non-recursive approach for the color covariance matrix eigenvectors detection. The new algorithm surpasses the existing similar algorithms in its lower computational complexity, which is a prerequisite for fast color segmentation or for adaptive coding of color images aimed at real time applications.

Keywords: Karhunen-Loève transform, color transforms, color space models, color covariance matrix, eigenvalues and eigenvectors, angles of Euler rotation, color image compression.

1 Introduction

The methods for color image space transform recently attract significant interest because they influence the efficiency of the processing aimed at the information redundancy reduction and color features extraction. Many attempts have been made to model the color perception by researchers working in various fields: psychology, computer vision, image processing and retrieval, computer graphics, etc. The color spaces used in image processing are derived from visual system models, adopted from technical domains or developed especially for image processing. The commonly used color space for image representation is based on RGB, XYZ, YCbCr, YUV, YCoCg, Lab, HSV/HSL, etc. color models [1-5]. All these color transform techniques do not depend on the image content. Unlike them, the Karhunen-Loeve Transform (KLT) [6] highly depends on the image content. The

Roumen Kountchev
Technical University – Sofia, Department of Radio Communications and Video Technologies, Boul. Kl. Ohridsky 8, Sofia 1000, Bulgaria
e-mail: rkountch@tu-sofia.bg

Roumiana Kountcheva
T&K Engineering Co. Mladost 3, POB12, Sofia 1712, Bulgaria
e-mail: kountcheva_r@yahoo.com

K. Nakamatsu et al. (Eds.): New Advan. in Intel. Decision Techno., SCI 199, pp. 171–182.
springerlink.com

KLT is utilized as a tool to eliminate the image redundancy, because the transformation components are highly uncorrelated. The KLT has found many applications in traditional fields such as communications [7-9] and computer vision. In computer vision, it is used for a variety of tasks such as image segmentation, face and object recognition, motion estimation, object tracking, etc. [10-13]. The KLT is however used infrequently as it is dependent on the image statistics, i.e. when the statistics change the KLT matrix should be changed as well. Because of this signal dependence, general fast algorithm is not developed. Additional disadvantage is its higher computational complexity in comparison with the deterministic image color space transforms. Some solutions of the problem have already been proposed. The basic methods used for the matrix eigenvectors calculation are given in [14]. One or the relatively simple methods is the iterative approach proposed by Jacobi. In accordance with it, the KLT matrix is presented as a product of rotation matrices, which consecutively rotate the image vector around the corresponding coordinate axis in the vector space. While this technique is quite simple, for big matrices it can take a large number of calculations. A more efficient approach for larger, symmetric matrices divides the problem into two stages. The Householder algorithm can first be applied to reduce a symmetric matrix into a tridiagonal form in a finite number of steps. Once the matrix is in this simpler form, an iterative method such as QR factorization (the matrix is represented by the product of upper triangular and orthogonal matrices) can be used to generate the eigenvalues and eigenvectors. The advantage of this approach is that the factorization of the simplified tridiagonal matrix requires fewness iterations than the Jacobi method. Significant interest attracted the iterative methods for principal components extraction with neural networks which do not require the calculation of a covariance matrix [15-17]. These techniques update the estimate of the eigenvectors for each input training vector. While these algorithms have some advantages over covariance-based methods, there are still some concerns over stability and convergence [18]. In particular, analytical solution for the components of the covariance matrix eigenvectors exists for the case when the color vectors depict first order stationary Markov process [6].

The goal of this work is to present a simplified method for the calculation of the KLT matrix for the RGB image color space. The paper is arranged as follows: section 2 introduces the principle of the direct calculation of the KLT matrix; in section 3 is evaluated the computational complexity of the new method and are given some results obtained by means of the method modeling and the comparison with the determined transform YCbCr; section 4 is the Conclusion.

2 Direct Calculation of the KLT Matrix

The color of every pixel in the digital image is represented in the color space by the vector $\vec{C} = [C_1, C_2, C_3]^t$, whose coordinates (C_1, C_2, C_3) correspond to the chosen primary colors (for example, RGB, etc.). The general algorithm for efficient coding of digital color images based on preliminary color space transform comprises the following basic operations:

1. Direct (linear or nonlinear) transform of the vector $\vec{C}$ into a new color space aimed to obtain maximum uncorrelated components. When linear transforms are used, the corresponding transformed color vector $\vec{L}=[L_1,L_2,L_3]^t$ is defined by the relation $\vec{L}=[T]\vec{C}$, where $[T]$ is the color transform matrix of size 3×3;

2. Coding of the transformed vector $\vec{L}$ components in correspondence with the relations $L_1^q=\psi_1(L_1),\ L_2^q=\psi_2(L_2),\ L_3^q=\psi_3(L_3)$ were $\psi_1(*), \psi_2(*)$ and $\psi_3(*)$ are functions, which correspond to the selected coding method for every component (aimed at the reduction of its psycho-visual and/or statistical redundancy). As a result is obtained the coded vector $\vec{L}_q=\psi(\vec{L})=\lfloor L_1^q,L_2^q,L_3^q \rfloor^t$, whose components are transferred to the decoder;

3. Decoding of the vector components in correspondence with the relations $L_1'=\psi_1^{-1}(L_1^q),\ L_2'=\psi_2^{-1}(L_2^q),\ L_3'=\psi_3^{-1}(L_3^q)$, where $\psi_1^{-1}(*), \psi_2^{-1}(*)$ and $\psi_3^{-1}(*)$ are the inverse transform functions. As a result is obtained the vector $\vec{L}'$;

4. Inverse transform of the decoded vector $\vec{L}'=[L_1',L_2',L_3']^t$. When orthogonal transforms are used, the restored color vector $\vec{C}'=[C_1',C_2',C_3']^t$ is defined by the relation $\vec{C}'=[T]^{-1}\vec{L}'$, where $[T]^{-1}$ is the inverse transform matrix of size 3×3.

The choice of the color space transform depends on the primary colors and the restored image quality, the compression ratio and the computational complexity required. In order to obtain high efficiency of the color image coding the components of the transformed color vector $\vec{L}$ for every pixel should be uncorrelated. This requirement is satisfied by the KLT model only.

In correspondence with this model the RGB color vector for the s^{th} pixel $\vec{C}_s=[R_s,G_s,B_s]^t$ is transformed into the vector $\vec{L}_s=[L_{1s},L_{2s},L_{3s}]^t$ using the matrix $[\Phi]$ of the linear orthogonal KLT. The elements of the matrix Φ_{ij} are defined by the statistical characteristics of the image pixels colors and could be calculated in the way described below. The covariance color matrix $[K_C]$ of size 3×3, is calculated first:

$$[K_C]=\frac{1}{S}\sum_{s=1}^{S}(\vec{C}_s\vec{C}_s^t)-\vec{m}_c\vec{m}_c^t=\begin{bmatrix} k_{11} & k_{12} & k_{13}\\ k_{21} & k_{22} & k_{23}\\ k_{31} & k_{32} & k_{33}\end{bmatrix}, \tag{1}$$

where $\vec{m}_C=[\overline{R},\overline{G},\overline{B}]^t$ is the mean color vector. Let $\overline{x}=E(x_s)=\frac{1}{S}\sum_{s=1}^{S}x_s$ is the operator for the calculation of the mean value of x_s, for $s = 1, 2, \ldots, S$. Then the elements of the vector $\vec{m}_c$ and of the matrix $[K_C]$ could be represented as follows:

$$\overline{R} = E(R_s), \quad \overline{G} = E(R_s), \quad \overline{B} = E(B_s), \tag{2}$$

$$k_{11} = k_1 = E(R_s^2) - (\overline{R})^2,\ k_{22} = k_2 = E(G_s^2) - (\overline{G})^2,\ k_{33} = k_3 = E(B_s^2) - (\overline{B})^2, \tag{3}$$

$$k_{12} = k_{21} = k_4 = E(R_s G_s) - (\overline{R})(\overline{G}), \quad k_{23} = k_{32} = k_6 = E(G_s B_s) - (\overline{G})(\overline{B}), \tag{4}$$

$$k_{13} = k_{31} = k_5 = E(R_s G_s) - (\overline{R})(\overline{G}). \tag{5}$$

Here $S = M \times N$ is the number of the pixels in the image with components $R_s\ G_s\ B_s$, whose mean values are correspondingly $\overline{R},\ \overline{G},\ \overline{B}$.

In this work below is presented one new approach for the calculation of the eigenvalues and eigenvectors of the covariance matrix $[K_C]$. The eigenvalues $\lambda_1, \lambda_2, \lambda_3$ of the matrix $[K_C]$ are the solution of its characteristic equation:

$$det|\, k_{ij} - \lambda \delta_{ij}\, | = \lambda^3 + a\lambda^2 + b\lambda + c = 0, \tag{6}$$

where:

$$\delta_{ij} = \begin{cases} 1, & i = j, \\ 0, & i \neq j. \end{cases} \quad \begin{aligned} & a = -(k_1 + k_2 + k_3),\ \ b = k_1 k_2 + k_1 k_3 + k_2 k_3 - (k_4^2 + k_5^2 + k_6^2), \\ & c = k_1 k_6^2 + k_2 k_5^2 + k_3 k_4^2 - (k_1 k_2 k_3 + 2 k_4 k_5 k_6), \end{aligned} \tag{7}$$

The matrix $[K_C]$ is symmetrical and its eigenvalues are always real numbers. They can be defined using the Cardano relations [19] for the "casus irreducibilis" (or the so-called "trigonometric solution"):

$$\lambda_1 = 2\sqrt{\frac{|p|}{3}}\cos\left(\frac{\varphi}{3}\right) - \frac{a}{3};\ \lambda_2 = -2\sqrt{\frac{|p|}{3}}\cos\left(\frac{\varphi + \pi}{3}\right) - \frac{a}{3};\ \lambda_3 = -2\sqrt{\frac{|p|}{3}}\cos\left(\frac{\varphi - \pi}{3}\right) - \tag{8}$$
$$\text{for } \lambda_1 \geq \lambda_2 \geq \lambda_3 \geq 0,$$

$$\varphi = \arccos\left[-q/2 \Big/ \sqrt{(|\, p\, |/3)^3}\, \right],\ \ q = 2(a/3)^3 - (ab)/3 + c,\ \ p = -(a^2/3) + b \cdot \tag{9}$$

The eigenvectors $\vec{\Phi}_1, \vec{\Phi}_2, \vec{\Phi}_3$ of the covariance matrix $[K_C]$ are the solution of the set of equations:

$$[K_C]\, \vec{\Phi}_m = \lambda_m \vec{\Phi}_m \quad \text{and} \quad \left|\vec{\Phi}_m\right|^2 = \sum_{i=1}^{3} \Phi_{mi}^2 = 1 \quad \text{for } m = 1, 2, 3. \tag{10}$$

The last equation derives from the conditions for orthogonality and normalization of the obtained eigenvectors:

$$\vec{\Phi}_s^t \vec{\Phi}_k = \sum_{i=1}^{3} \Phi_{is} \Phi_{ik} = \begin{cases} 1 \ \ for \ \ s = k\,; \\ 0 \ \ for \ \ s \neq k\,. \end{cases} \quad \text{for } \ s,\, k = 1,2,3. \tag{11}$$

Solving Eq. (10) are defined the components of the m^{th} eigenvector $\vec{\Phi}_m = [\Phi_{m1}, \Phi_{m2}, \Phi_{m3}]^t$, which corresponds to the eigenvalue λ_m (Eq. 8). Then:

$$\Phi_{m1} = A_m / P_m;\ \Phi_{m2} = B_m / P_m;\ \Phi_{m3} = D_m / P_m \qquad \text{for } \ m = 1,2,3 \tag{12}$$

$$A_m = (k_3 - \lambda_m)[k_5 (k_2 - \lambda_m) - k_4 k_6\,],\ \ \mathrm{B_m} = (k_3 - \lambda_m)[k_6 (k_1 - \lambda_m) - k_4 k_5], \tag{13}$$

$$D_m = k_6 [2 k_4 k_5 - k_6 (k_1 - \lambda_m)] - k_5^2 (k_2 - \lambda_m),\ \ P_m = \sqrt{A_m^2 + B_m^2 + D_m^2} \neq 0. \tag{14}$$

The matrix $[\Phi]$ whose rows comprise the components Φ_{ms} of the eigenvectors $\vec{\Phi}_m$ is:

$$[\Phi] = \begin{bmatrix} \vec{\Phi}_1^t \\ \vec{\Phi}_2^t \\ \vec{\Phi}_3^t \end{bmatrix} = \begin{bmatrix} \Phi_{11} & \Phi_{12} & \Phi_{13} \\ \Phi_{21} & \Phi_{22} & \Phi_{23} \\ \Phi_{31} & \Phi_{32} & \Phi_{33} \end{bmatrix} \ \text{for } m = 1,2,3 \tag{15}$$

The color vector $\vec{C}_s = [R_s, G_s, B_s]^t$ is then transformed into the vector $\vec{L}_s = [L_{1s}, L_{2s}, L_{3s}]^t$ using the direct KLT:

$$\begin{bmatrix} L_{1s} \\ L_{2s} \\ L_{3s} \end{bmatrix} = \begin{bmatrix} \Phi_{11} & \Phi_{12} & \Phi_{13} \\ \Phi_{21} & \Phi_{22} & \Phi_{23} \\ \Phi_{31} & \Phi_{32} & \Phi_{33} \end{bmatrix} \left(\begin{bmatrix} R_s \\ G_s \\ B_s \end{bmatrix} - \begin{bmatrix} \overline{R} \\ \overline{G} \\ \overline{B} \end{bmatrix} \right) \ \text{for } \ s = 1,\, 2, \ldots,\, S. \tag{16}$$

The components of the vector $\vec{L}_s = [L_{1s}, L_{2s}, L_{3s}]^t$ could be coded using various methods (decimation and interpolation, filtration, orthogonal transforms, quantization, etc.) in correspondence with relations $L_{1s}^q = \psi_1(L_{1s})$, $L_{2s}^q = \psi_2(L_{2s})$, $L_{3s}^q = \psi_3(L_{3s})$ and then is obtained the coded vector $\vec{L}_s^q = \psi(\vec{L}_s) = [\psi_1(L_{1s}), \psi_2(L_{2s}), \psi_3(L_{3s})]^t$.

For the restoration of the vector $\vec{L}_s^q$ components, are applied inverse functions in correspondence to relations $\hat{L}_{1s} = \psi_1^{-1}(L_{1s}^q)$, $\hat{L}_{2s} = \psi_2^{-1}(L_{2s}^q)$, $\hat{L}_{3s} = \psi_3^{-1}(L_{3s}^q)$ and is obtained the decoded vector $\vec{\hat{L}}_s = \left[\hat{L}_{1s}, \hat{L}_{2s}, \hat{L}_{3s}\right]^t$. Using the inverse KLT the vector $\vec{\hat{L}}_s$ is transformed into the restored color vector $\vec{\hat{C}}_s = \left[\hat{R}_s, \hat{G}_s, \hat{B}_s\right]^t$:

$$\begin{bmatrix} \hat{R}_s \\ \hat{G}_s \\ \hat{B}_s \end{bmatrix} = \begin{bmatrix} \Phi_{11} & \Phi_{21} & \Phi_{31} \\ \Phi_{12} & \Phi_{22} & \Phi_{32} \\ \Phi_{13} & \Phi_{23} & \Phi_{33} \end{bmatrix} \begin{bmatrix} \hat{L}_{1s} \\ \hat{L}_{2s} \\ \hat{L}_{3s} \end{bmatrix} + \begin{bmatrix} \overline{R} \\ \overline{G} \\ \overline{B} \end{bmatrix} \text{ for } s = 1, 2, \ldots, S, \tag{17}$$

where

$$[\Phi]^{-1} = [\Phi]^t = \left[\vec{\Phi}_1, \vec{\Phi}_2, \vec{\Phi}_3\right] = \begin{bmatrix} \Phi_{11} & \Phi_{21} & \Phi_{31} \\ \Phi_{12} & \Phi_{22} & \Phi_{32} \\ \Phi_{13} & \Phi_{23} & \Phi_{33} \end{bmatrix} \tag{18}$$

is the matrix of the inverse KLT.
Unlike the deterministic transforms, the restoration of the primary color vectors $\vec{\hat{C}}_s = \left[\hat{R}_s, \hat{G}_s, \hat{B}_s\right]^t$ with the inverse KLT (Eq. 17) needs not only the transformed color vectors $\vec{L}_s = \left[L_{1s}, L_{2s}, L_{3s}\right]^t$, but the elements Φ_{ij} of the matrix $[\Phi]$ as well. The number of these elements is reduced when the ability of the matrix $[\Phi]$ to represent the transform of the initial color space in correspondence with Eq. 17 as three rotations around each coordinate axis *R, G* and *B*, is used. The three angles of the Euler rotation (α, β, γ) define the position of the transform coordinate axes (L_1, L_2, L_3) in respect to the original color space. Using this quality of the matrix $[\Phi]$ it is represented by the product of the following 3 rotation matrices for the axes *(R, G, B)* [19]:

$$[\Phi] = \begin{bmatrix} \Phi_{11} & \Phi_{12} & \Phi_{13} \\ \Phi_{21} & \Phi_{22} & \Phi_{23} \\ \Phi_{31} & \Phi_{32} & \Phi_{33} \end{bmatrix} = [\Phi_3(\alpha)][\Phi_2(\beta)][\Phi_3(\gamma)] = [\Phi_{32}(\alpha, \beta, \gamma)] \tag{19}$$

where

$$[\Phi_3(\alpha)] = \begin{bmatrix} \cos\alpha & -\sin\alpha & 0 \\ \sin\alpha & \cos\alpha & 0 \\ 0 & 0 & 1 \end{bmatrix}; \quad [\Phi_2(\beta)] = \begin{bmatrix} \cos\beta & 0 & -\sin\beta \\ 0 & 1 & 0 \\ \sin\beta & 0 & \cos\beta \end{bmatrix}; \tag{20}$$

$$[\Phi_3(\gamma)] = \begin{bmatrix} \cos\gamma & -\sin\gamma & 0 \\ \sin\gamma & \cos\gamma & 0 \\ 0 & 0 & 1 \end{bmatrix}$$

$$\begin{aligned} &\Phi_{11} = \cos\alpha\cos\beta\cos\gamma - \sin\alpha\sin\gamma;\ \Phi_{12} = -(\cos\alpha\cos\beta\sin\gamma + \sin\alpha\cos\gamma); \\ &\Phi_{21} = \sin\alpha\cos\beta\cos\gamma + \cos\alpha\sin\gamma;\ \Phi_{22} = -\sin\alpha\cos\beta\sin\gamma + \cos\alpha\cos\gamma; \\ &\Phi_{13} = -\cos\alpha\sin\beta;\ \Phi_{23} = -\sin\alpha\sin\beta;\ \Phi_{31} = \sin\beta\cos\gamma;\ \Phi_{32} = -\sin\beta\sin\gamma; \\ &\Phi_{33} = \cos\beta. \end{aligned} \tag{21}$$

The determinant of the KLT matrix should be checked carefully, since the Euler theorem applies only to matrices with a determinant of 1, but the determinant of the KLT matrix may be -1 as well. In this case, one of the rows should be inverted to produce the matrix of determinant 1 prior to decomposition. The matrix of the inverse KLT in this case is defined by the relation:

$$[\Phi]^{-1} = [\Phi_3(-\gamma)][\Phi_2(-\beta)][\Phi_3(-\alpha)] \tag{22}$$

Hence, in order to define $[\Phi]^{-1}$ for the decoding are needed the Euler angles α, β and γ only. These angles are calculated using Eqs. (19 - 21), when the elements of the matrix $[\Phi]$ are known:

$$\alpha = -\arcsin\left(\frac{\Phi_{23}}{\sqrt{1-\Phi_{33}^2}}\right);\quad \beta = arccos(\Phi_{33});\quad \gamma = \arccos\left(\frac{\Phi_{31}}{\sqrt{1-\Phi_{33}^2}}\right). \tag{23}$$

The elements of the matrix $[\Phi]^{-1}$ are then restored using Eqs. (21-23) and knowing the angles α, β and γ. As a result to the decoder are transferred the values of angles α, β, γ only, instead of the 9 elements of the matrix $[\Phi]^{-1}$, i.e. the number of needed coefficients is 3 times smaller.

3 Estimation of the Enhanced KL Color Transform

On the basis of Eqs. (1-15) used for the direct calculation of the eigenvalues and eigenvectors of the color covariance matrix and the Euler angles (Eq. 23), was developed the algorithm for enhanced KL image color space transform. It offers acceleration of the transform calculations because of the reduced number of mathematical operations in comparison with the numerical methods used for the general approach with covariance matrix of arbitrary size [6, 19].The computational complexity of the new algorithm was compared with that of the QR algorithm for calculation of the eigenvalues $\lambda_1, \lambda_2, \lambda_3$. The number of the operation needed for their calculation for a square matrix of size $n \times n$ when QR decomposition of the matrix in the step k is used [20] is given in Table 1.

Table 1 Computational complexity of the QR decomposition in the *k*-th step

Operation	Number of operations
multiplications	$2(n - k + 1)^2$
additions	$(n - k + 1)^2 + (n - k + 1)(n - k) + 2$
divisions	1
square roots	1

Summing these numbers over the $(n-1)$ steps for equal weight of the operations in Table 1 is obtained:

$$SS(n) = \sum_{k=1}^{n-1}[3(n-k+1)^2 + (n-k+1)(n-k) + 4] = (n-1)(\frac{4}{3}n^2 + \frac{17}{6}n + 7)\,. \tag{24}$$

Then, for $n=3$ from Eq. (24) follows that $SS(3) = 55$.

For the case with the direct calculation of $\lambda_1, \lambda_2, \lambda_3$ using Eqs. (7-9) is obtained:

$$SS(3) = 28 \; multiplications + 19 \; additions = 47. \tag{25}$$

Hence, the computational complexity for the direct calculation of the matrix $[K_C]$ eigenvalues in respect of the QR decomposition is 14.5 % lower. Further reduction is obtained as a result of the direct calculation of the $[K_C]$ eigenvectors in accordance with Eqs. (10-14).

The efficiency of the new method regarding the bit-rate and the restored image quality was evaluated for RGB color images (24 bpp) of various sizes. For the evaluation was used DCT-based JPEG-like compression algorithm. Some of the results obtained are given in Table 2. It is obvious that for same (or very close) quality the bit-rate obtained with the KL transform is lower (in average more than 10%).

For the evaluation of the influence of the new approach on the color components' energy distribution was used a database of 4 image groups. Some of the test images are shown in Fig.1: deserts and beaches (a, b); forest (c, d); interiors (e, f) and city (g, h). The goal of the experiments was to prove the efficiency of the proposed algorithm: the energy concentration mainly in one component, the decorrelation of the three components and the MSE minimization.

The algorithm performance was also compared with that of YCbCr and HSV color transforms. For this the relative energy for each color component of the transformed image was calculated. The energies concentrated in each of the three

Table 2 Comparative results for the bit-rate/PSNR relation for the direct KLT approach versus YCbCr (Rec. 601.2) for a group of RGB color test images (24 bpp)

No.	Image (pixels)	KLT		YCbCr	
		Bit-rate bpp	PSNR dB	Bit-rate bpp	PSNR dB
1	Amber (88x128)	1,36	29,06	1,42	29,05
2	Chris (88x128)	1,46	28,99	1,53	28,98
3	Canyon (600x480)	1,63	26,37	1,69	26,37
4	Lena (512x512)	1,11	30,90	1,48	30,85
5	Myanmar (1024x768)	1,45	26,10	1,50	26,09
6	Phong (800x608)	0,14	37,36	0,18	37,68

transformed components were represented as percentage of their sum. The results obtained for the energy distribution within individual image groups were very close. In each group was observed that the principal eigenvector of each image is close to the principal eigenvector of the group. So instead of calculating a KLT for each image of each group we could calculate a single transform for all images in each group. The energy distribution for one of the tested image groups (forest) is given in Table 3.

The color transforms YCbCr and HSV were performed for same database of color images and the relative power for each of the three components of the color transforms was calculated. In Fig. 2a is shown the relation of the relative energies of the first and the second component and Fig. 2b represents the relation of the relative energies of the first and the third component. The graphics show that the relationship between the energies of the first and the second component for the color transforms YCbCr and HSV is close but this is not the same for the KL color transform. As opposed to the other color transforms the energies of the three bands are strongly uncorrelated: most energy is concentrated in the first component; the energies in the second and third component are much smaller. From the data given in Table 2 for the tested image groups is assumed that the relation between the components in the K-L color space is roughly 4:2:1, this means that the first component can be left untouched, the second is twice as small as the original and the third is four times as small as the original.

a) b) c) d) e) f) g) h)

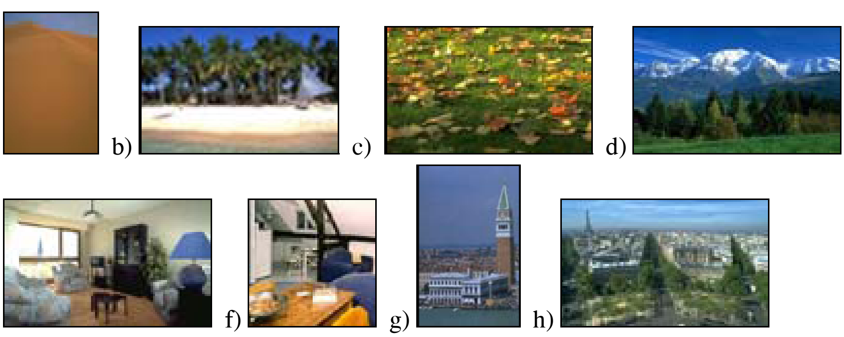

Fig. 1 Some of the test images used for the experiments

Table 3 Energy distribution of the components L_1, L_2, L_3 for each image group

Group	Energy of L_1 [%]	Energy of L_2 [%]	Energy of L_3 [%]
Desert/Beach	64.30	18.40	17.30
Forest	76.99	21.63	1.38
Indoor	48.66	35.51	15.82
City	58.53	23.66	17.81

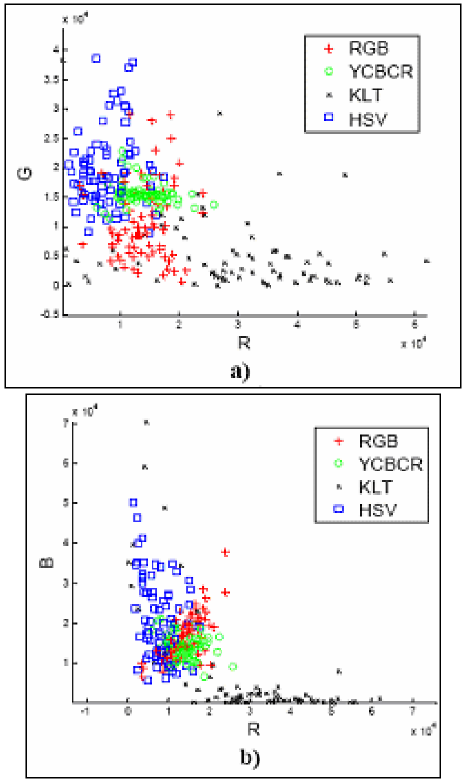

Fig. 2 Distribution of the color components' energies

4 Conclusion

The presented algorithm for direct calculation of the KLT matrix for the RGB image color space does not require the use of numerical methods for the calculation of the eigenvalues and eigenvectors of the color covariance matrix. Further enhancement of the KLT algorithm performance can be achieved if the principles of distributed arithmetic are used. More experiments could be performed concerning the use of the integer numbers arithmetic for the presented approach.

The experimental results obtained confirmed the direct KLT efficiency: it offers lower computational complexity and bit rate for same quality. Another advantage is that the algorithm is universal in respect of the initial color space.

One more advantage is that the algorithm permits the corresponding transform matrices for some large image classes to be calculated in advance. Then, on the basis of the color histogram analysis the processed images could be easily classified and the most suitable matrix to be used.

The main application areas of the direct KL color transform, presented above, are:

- fast color segmentation for automatic target recognition and image classification (image data mining);
- adaptive and more efficient coding of color images.

Acknowledgement. This paper was supported by the National Fund for Scientific Research of the Bulgarian Ministry of Education and Science (Contr. VU-I 305/2007)

References

1. Fairchild, M.: Color and Image Appearance Models. John Wiley & Sons, Chichester (2005)
2. Pratt, W.: Digital Image Processing. Wiley Interscience, New York (2007)
3. Gonzalez, R., Wood, R.: Digital Image Processing. Prentice-Hall, Englewood Cliffs (2001)
4. Malvar, H., Sullivan, G.: Transform, Scaling and Color Space Impact of Professional Extensions, ISO/IEC JTC1/SC29/WG11 and ITU-T SG16 Q.6 Document JVT-H031, Geneva (2003)
5. Hoffmann, G.: CIELab Color Space, Wikipedia, the free encyclopedia.mht
6. Dony, R.: The Transform and Data Compression Handbook. In: Rao, K., Yip, P. (eds.) Karhunen-Loève Transform. CRC Press LLC, Boca Raton (2001)
7. Carevic, D., Caelli, T.: Region based coding of color images using K-L transform. Graphical Models and Image Processing 59(1), 27–38 (1997)
8. Hao, P., Shi, Q.: Reversible Integer KLT for progressive-to-lossless compression of multiple component images. In: ICIP, vol. 1, pp. 633–636 (2003)
9. Chen, Y., Hao, P., Dang, A.: Optimal transform in perceptually uniform color space and its application in image coding. In: Campilho, A.C., Kamel, M.S. (eds.) ICIAR 2004. LNCS, vol. 3211, pp. 269–276. Springer, Heidelberg (2004)
10. Devaux, J., Gouton, P., Truchetet, F.: Karhunen-Loeve transform applied to region-based segmentation of color aerial images. Optical Engineering 40(7), 1302–1308 (2001)
11. Ionita, M., Corcoran, P.: Benefits of Using Decorrelated Color Information for Face Segmentation/Tracking. Advances in Optical Technologies (2008) article ID 583687
12. Kouassi, R., Devaux, J., Gouton, P., Paindavoine, M.: Application of the Karhunen-Loeve transform for natural color images analysis. In: Proceedings of the 31st Asilomar Conference on Signals, Systems & Computers (ACSSC 1997), USA, vol. 2, pp. 1740–1744 (1997)
13. Devaux, J., Gouton, P., Truchetet, F.: Aerial color image segmentation by Karhunen-Loeve transform. In: Proceedings of the 15th International Conference on Pattern Recognition (ICPR 2000), Spain, vol. 1, pp. 309–312 (2000)
14. Jolliffe, I.: Principal Component Analysis, 2nd edn. Springer, NY (2002)

15. Dony, R., Haykin, S.: Optimally adaptive transform coding. IEEE Trans. Image Processing 4(10), 1358–1370 (1995)
16. Gorban, A., Kegl, B., Wunsch, D., Zinovyev, A. (eds.): Principal Manifolds for Data Visualisation and Dimension Reduction. LNCSE, vol. 58. Springer, Berlin (2007)
17. Diamantaras, K., Kung, S.: Principal Component Neural Networks: Theory and Applications. John Wiley & Sons, New York (1996)
18. Solo, V., Kong, X.: Performance analysis of adaptive eigen analysis algorithms. IEEE Trans. Signal Processing 46(3), 636–645 (1998)
19. Korn, G., Korn, T.: Mathematical Handbook for Scientists and Engineers. Mc Graw-Hill Book Company, NY (2000)
20. QR decomposition - Wikipedia, the free encyclopedia.mht